

Huiting Lin^{1,*},
Nicholus Tayari Akankwasa²,
Jun Wang²,
Chuyang Zhang¹

Simulation of the Effect of Geometric Parameters of the Fibre Transport Channel in Open-End Rotor Spinning

DOI: 10.5604/01.3001.0012.9987

¹ Quanzhou Normal University,
College of Textiles and Apparel,
Quanzhou 362000, China
*e-mail: linht1218@126.com

² Donghua University,
College of Textile,
Shanghai, China

Abstract

The airflow field in a fibre transport channel is crucial as it affects the fibre configuration significantly and, consequently, the yarn properties. Geometric parameters are found to be critical in influencing airflow characteristics. 3D finite volume computations were adopted to evaluate the effects of geometric parameters of the transport channel on airflow characteristics. A bypass channel for extra air supply into the transport channel was also evaluated. The results reveal that the transport channel inlet area has a more significant impact on the vortices generated at the channel inlet than the transport channel length. Either increasing the transport channel length or decreasing the transport inlet area can reduce the vortices but cannot eliminate them. By adopting a bypass channel, the vortices are reduced significantly and the air velocity at the transport channel inlet, especially in the fibre separation area, is increased.

Key words: fibre transport channel, airflow, simulation, rotor spinning, bypass channel.

Introduction

The nature of the rotor spinning system is a process of separating the fibre strands into individual fibres and collecting them again in the rotor groove to form a yarn [1]. During the process of fibre separation, transportation and gathering, a loss of fibre orientation and straightness often occurs due to possible adverse airflow, which would lower the rotor spun yarn tenacity to some extent [2-4]. The airflow characteristics in the rotor spinning channel are closely related to the geometric and spinning operation parameters, such as the dimensions and shape of the transport channel and rotor [5], the speed of the rotor and opening roller [6, 7], and the rotor outlet pressure [6]. It is essential that these parameters are adjusted to suitable values to obtain a favourable airflow environment for fibre transportation.

During the past decades, researchers have focused on studying the mechanisms of rotor spun yarn formation and the optimisation of spinning and geometric parameters. Koç and Lawrence [8] investigated the mechanics of yarn twist insertion and the formation of wrapper fibres in the rotor, which is the primary cause of low yarn tenacity. Among other factors, the hooked fibres generated during the opening and transportation processes also lead to the low tenacity of the rotor spun yarn. Lawrence and Chen [9, 10] reported that compared to the circular cross-section of the transfer channel inlet, a narrow rectangular one was more conducive to fibre straightness. In Eskandarnajad's thesis [11], the transport channel was

modified in order to reduce fibre flicking over the outer wall of the transport channel and to prevent fibre displacement at the transport channel inlet. Recently researchers modified the transport channel for the purpose of improving rotor spun yarn properties. Seyed et al. [12] evaluated the effect of eight different transport channel outlet slots on yarn properties and claimed that reducing the slot width could increase the yarn tenacity. Wang et al. [13] designed a dual feed rotor spinning box with a dual feed roller and transport channel. Later on, Akankwasa et al. [14] numerically simulated the internal airflows in the dual feed rotor spinning box, and their results showed that the velocity magnitude and pressure in the dual-feed unit adopted an even pattern. Moreover the dual-feed spun yarns possessed superior quality compared to conventional yarns [15].

Kong and Platfoot [5] indicated that there was a recirculation zone generated at the transport channel inlet. Zhang et al. [16] stated that decreasing the fibre separation area could improve fibre orientation due to the reduction of recirculation. It is possible to reduce the flow vortices via optimising the transport channel geometric parameters. Lin et al. [17] developed a three-dimensional CFD model of the rotor spinning unit to evaluate the airflow characteristics in the transfer channel, and proposed a better design of the transfer channel with a rounded corner and a bypass channel. As a further exploration of our previous study, the current paper reports an evaluation of the influence of the characteristic number of the

transport channel on its airflow patterns and the possible improvement of yarn properties. Modifications of the transport channel generating no air vortices are further evaluated.

Theoretical and mathematical model

Rotor spinning geometric model

In this research, the computational domain is the spinning channel from the trash extraction chute to the rotor, including the opening roller chamber, transport channel, and yarn guiding mouth. Strictly based on the real model (JWF1612-2157A rotor spinning unit), the rotor spinning unit model with its main dimensions, which is developed in the Cartesian coordinate system, is illustrated in *Figure 1*. The origin is located at the bottom centre of the rotor, and the y -axis is perpendicular to the rotor bottom, on which the x - z plane is located. Because individual fibres are airborne when moving through the transport channel and the movement characteristic is similar to the fluid flow mechanism, we considered the effects of some geometrical parameters of the transport channel on the airflow characteristics.

As the characteristic number λ , which indicates the reducing degree of the transport channel along its length, is an important factor considered when designing the transport channel, it is mainly evaluated in this paper. The characteristic number λ is defined as:

$$\lambda = (S_{in}/S_{out})/L \quad (1)$$

Where, L is the transport channel length, and are the transport channel inlet and outlet areas, respectively. Accordingly the parameters evaluated in this study are presented in **Table 1**. For easy comparison, the transport channel outlet area is considered as a constant.

Governing equations and turbulence model

The airflow in the transport channel is assumed as a viscous, incompressible and isentropic turbulence flow. Based on mass conservation and momentum conservation, the governing equations are expressed as:

$$\text{div}(\rho \mathbf{u}) = 0 \quad (2)$$

$$\begin{aligned} \partial(\rho u_i) / \partial t + \text{div}(\rho \mathbf{u} u_i) = \\ = \text{div}(\mu \text{grad} u_i) - \partial p / \partial x_i + S_i \end{aligned} \quad (3)$$

Where, ρ is the fluid density, \mathbf{u} a velocity vector, u_i the velocity component of \mathbf{u} in the x_i direction, μ the dynamic viscosity, p pressure, and S_i is the general source term in the x_i direction.

As the Reynold's number in the transport channel is high [4], the turbulent model should be considered. In this study, the realisable $k-\varepsilon$ model is adopted, while the wall functions are used in the near-wall regions.

Boundary conditions

The boundary conditions employed throughout all simulations are as follows:
Opening roller speed: 6000 rpm, clockwise

Rotor speed: 100000 rpm, clockwise
Rotor outlet relative pressure: -7000 Pa
The trash extraction chute: 101000 Pa
The yarn guiding mouth: 101000 Pa
The solid walls: non-slip boundary condition

Numerical method

The whole computational domains are meshed into a mix of structured hexahedral cells and unstructured tetrahedral cells. The numerical models are finally calculated based on the Finite Volume Method and SIMPLEC algorithm. Grid independence tests are performed to guarantee the accuracy of the computations. All simulations are carried out using the FLUENT 14.5 package.

Results and discussions

According to **Equation (1)**, the characteristic number λ is related to both the

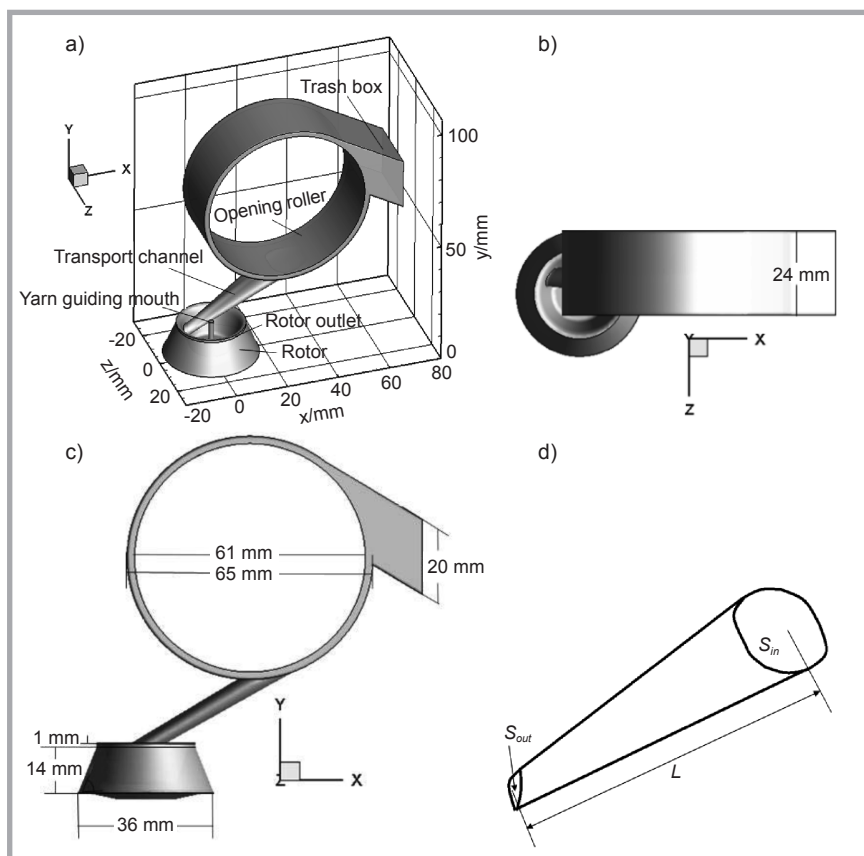


Figure 1. Geometrical profiles of the rotor spinning unit: a) 3-D model, b) -y direction, c) -z direction, d) transport channel.

Table 1. Parameters evaluated.

Case	1	2	3	4	5	6	7
λ	0.2	0.2	0.17	0.17	0.17	0.15	0.15
L/mm	44	37.5	44	37.5	50	44	50
S_{in}/mm^2	176	150	150	127.5	170	132	150

transport channel length L and transport channel inlet area S_{in} . Therefore the following three conditions are considered:
Condition I: S_{in} is kept constant, and therefore λ is changed with L
Condition II: L is kept as a constant, where λ is changed with S_{in}
Condition III: λ is a constant, while S_{in} and L are changed proportionally

Condition I: λ changed with L (S_{in} unchanged)

In cases 2, 3 and 7, the transport channel inlet area S_{in} remained constant, while the characteristic number decreased as the transport channel length L was increased. **Figure 2** presents the flow velocity streamlines at the transport channel inlet of these three cases.

As described in [6], the suction pump extracts the air inside the rotor, forming a negative pressure zone in it. Therefore

the external air flows into the spinning channel from the trash extraction chute. Due to the peculiar structure of the transport channel, vortices are generated on both sides of the transport channel inlet (see **Figure 2**), which would significantly influence the movement and orientation of the fibres inside the transport channel. The fibres are vulnerable to bending when coming into contact with the vortices. Or even more serious, the process of fibre peeling from the opening roller pins could be disturbed as it is possible for the fibres to be entangled among the vortices. In a cross section of the transport channel, the area containing no vortices is defined as the effective area for fibre transportation. It can be seen from **Figure 2** that the vortices decrease gradually as the transport channel length increases from 37.5 mm to 50 mm. This indicates that increasing the transport channel length can improve the airflow streamlines along

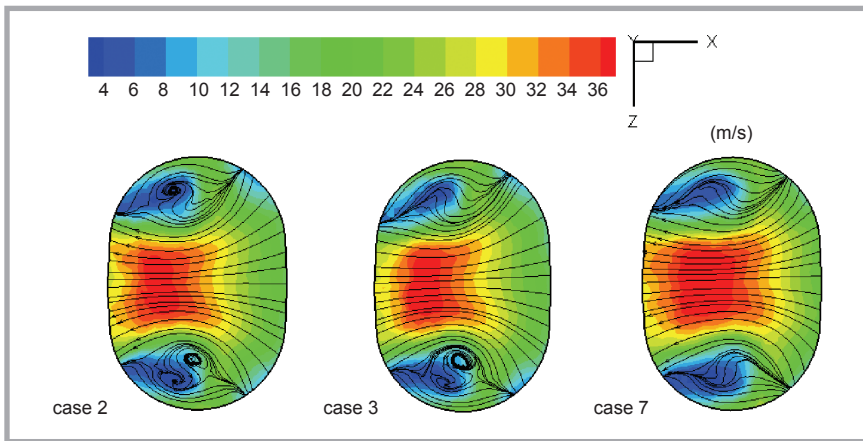


Figure 2. Flow velocity streamlines at the transport channel inlet (cross-section $y = 30$ mm) for different cases: case 2: $\lambda = 0.2$, $L = 37.5$ mm; case 3: $\lambda = 0.17$, $L = 44$ mm; case 7: $\lambda = 0.15$, $L = 50$ mm.

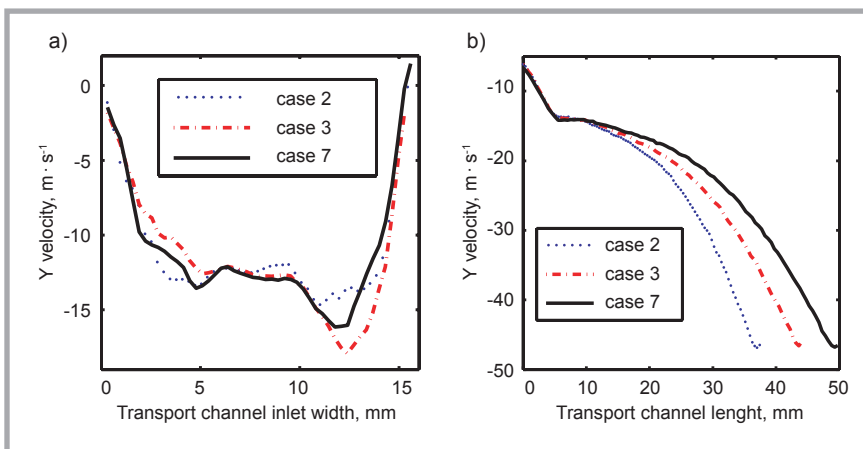


Figure 3. Effects of the transport channel length L on the transport channel Y velocity: a) along the centre line of the transport channel inlet cross section and b) along the transport channel length.

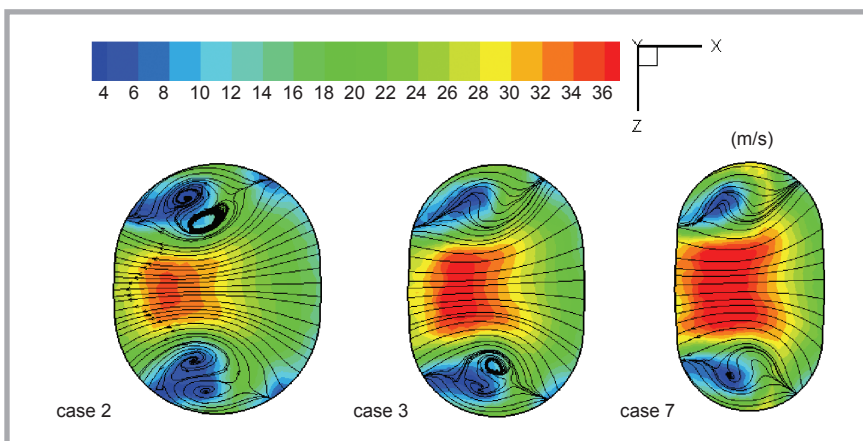


Figure 4. Flow velocity streamlines at the transport channel inlet (cross-section $y = 30$ mm) for different cases: case 1: $\lambda = 0.2$, $S_{in} = 176$ mm²; case 3: $\lambda = 0.17$, $S_{in} = 156$ mm²; case 6: $\lambda = 0.15$, $S_{in} = 132$ mm².

the transport channel, thus increasing the effective area. However, the impact of the transport channel length on the transport channel inlet velocity is small (see **Figures 2** and **3.a**). The transport channel inlet velocity in the centre region is

higher than that at the side of the channel, however, as the transport channel length increases, the velocities fluctuate slightly. From **Figure 3.b**, in the upper part of the transport channel, cases 2, 3 and 7 have the same air velocity, while in the lower

part the air velocity acceleration differs within three cases. With the increasing of the transport channel length, the velocity acceleration decreases since the Y velocity in the transport channel is the same, which is about 47 m/s. This indicates that for a shorter transport channel length, the individual fibre will have less time to finish its drawing process.

Condition II: λ changed with S_{in} (L unchanged)

The transport channel inlet area is an important factor which influences the fibre separation area. Cases 1, 3 and 6 evaluate the effect of the transport channel inlet area (176 mm², 156 mm² and 132 mm²) on the airflow dynamics of the transport channel.

As illustrated in **Figure 4**, when the transport channel inlet area increases to 176 mm², the vortices at the transport channel inlet increase significantly, while in case 6 ($S_{in} = 132$ mm²) the vortices are rather small. When considering the transport channel inlet velocity, it can be seen from **Figure 4** and **Figure 5.a** that the transport channel inlet area has a significant influence on the airflow dynamics. When increasing the transport channel inlet area from 132 mm² to 176 mm², a decrease in the ratio of the effective transportation area can be seen. Furthermore the air velocity of the centre area of the transport channel inlet as well as of its upper part is higher in case 6 than in cases 1 and 2 (see **Figure 5**). As described in [16], increasing the air velocity of the transport channel inlet is helpful for fibre removal from the opening roller pins and for maintaining its configuration. In **Figure 5.b**, the Y velocity in all the three cases experiences a sharp increase at the beginning and end of the transport channel, while in the middle part of the transport channel, the increase slows down. There is a slight difference in the velocity increase rate among the three cases; however, its influence on the fibre configuration may be smaller than that of the vortices generated at the transport channel inlet. Therefore among cases 1, 3 and 6, case 6 is more beneficial for keeping fibre straightness and, consequently, improving yarn properties.

Condition III: S_{in} and L changed simultaneously ($\lambda = 0.17$)

The characteristic number λ remains constant when the transport channel length L and inlet area S_{in} are adjusted proportionally. Cases 3, 4 and 5 compare the airflow

characteristic in the transport channel when the characteristic number λ is 0.17. The result is shown in **Figures 6** and **7**.

In **Figure 6**, it is seen that although the characteristic numbers of these three cases are the same, the airflow characteristics of the transport channels show different results. Case 5 shows larger vortices than those in cases 3 and 4; however, the difference in the vortices between cases 3 and 4 is small. The region with an air velocity of 30–36 m/s at the transport channel inlet increases when the transport channel inlet area decreases. The Y velocity distribution in cases 3, 4 and 5, illustrated in **Figure 7**, is similar to that shown in **Figures 3.b** and **5.b**. It is observed that with a small characteristic number (case 4), the Y velocity acceleration increases, and the fibre drawing process will be completed in a shorter time. So far from the three cases studied, when keeping the characteristic number as a constant, decreasing the transport channel length and inlet area simultaneously can be more favourable for improving the fibre configuration.

When considering the simulation results presented in **Figures 2** and **4**, and comparing them with those shown in **Figure 6**, it can be observed that the transport channel length L has a weaker influence on the airflow characteristics in the transport channel than the transport channel inlet area S_{in} . The variation between cases 3, 4 and 5 is similar to that of cases 1, 3 and 6, which is that the larger the transport channel inlet area S_{in} , the larger the vortices generated at the transport channel inlet. However, increasing the transport channel length does not reduce the adverse effect brought by the increase in the transport channel inlet area when comparing the velocity streamlines of cases 5 and 7. In general, it is recommended that the characteristic number be reduced in order to obtain a favourable airflow streamline.

It is the inherent nature of the transport channel to generate vortices. Changing the transport channel length or inlet area could reduce them but cannot eliminate them. According to a previous study, a better design of the transport channel with a rounded corner and bypass channel proposed can improve the transport channel airflow streamlines significantly [17]. As the dimensions of the rotor spinning unit are strictly the same with the real model, it can be further stated that only adopting a bypass channel as

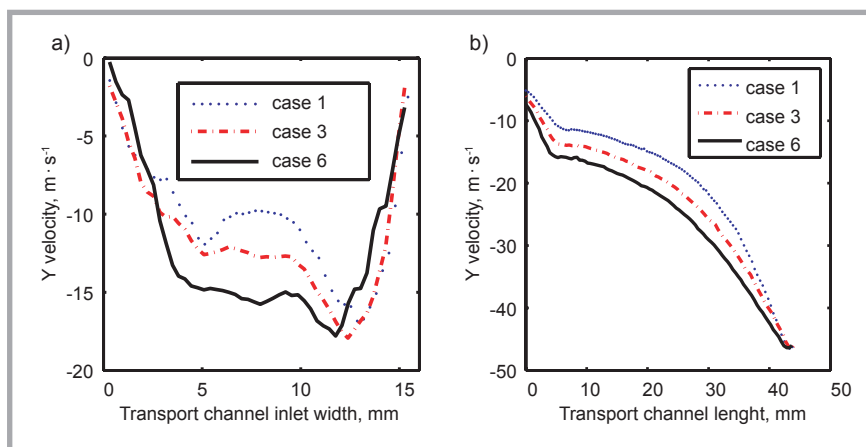


Figure 5. Effects of S_{in} on transport channel Y velocity: a) along the centre line of the transport channel inlet cross section and b) along the transport channel length.

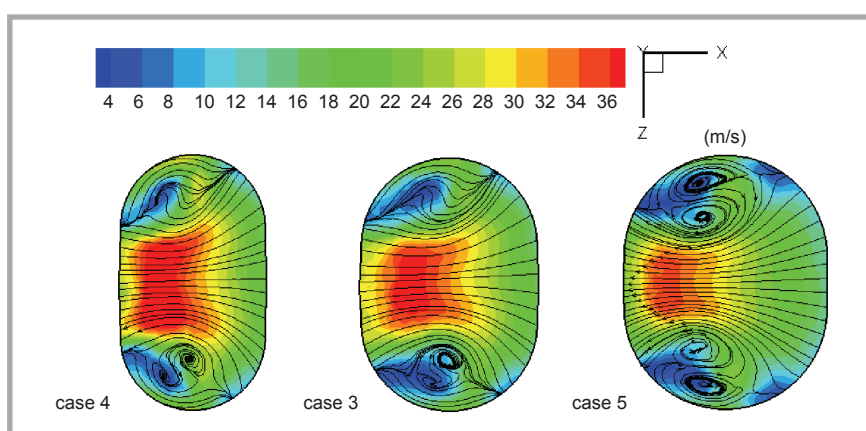


Figure 6. Flow velocity streamlines at the transport channel inlet (cross-section $y = 30$ mm) for different cases: case 4: $L = 37.5$ mm, $S_{in} = 127.5$ mm²; case 3: $L = 44$ mm, $S_{in} = 150$ mm²; case 5: $L = 50$ mm, $S_{in} = 170$ mm².

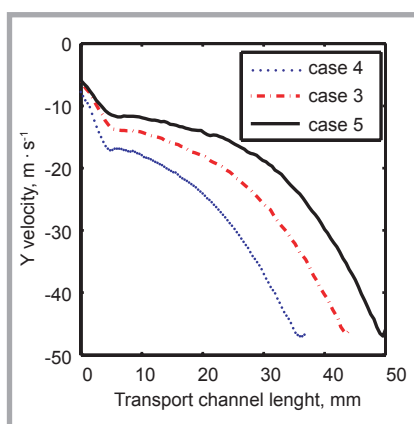


Figure 7. Y velocity distributions along the transport channel length for different cases.

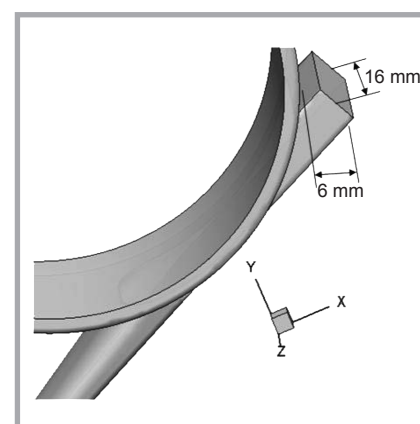


Figure 8. Transport channel with a bypass channel.

an external air supply channel could also achieve a relatively satisfactory effect. Therefore, in the following section, the effectiveness of the bypass channel is evaluated, and the variation in air velocities in the fibre separation area is particularly analysed.

Design of the bypass channel

Bypass channel structure

Figure 8 shows the geometrical structure of the bypass channel. It is located on the long side of the transport channel with its flow direction tangent to the transport channel wall. The inlet areas

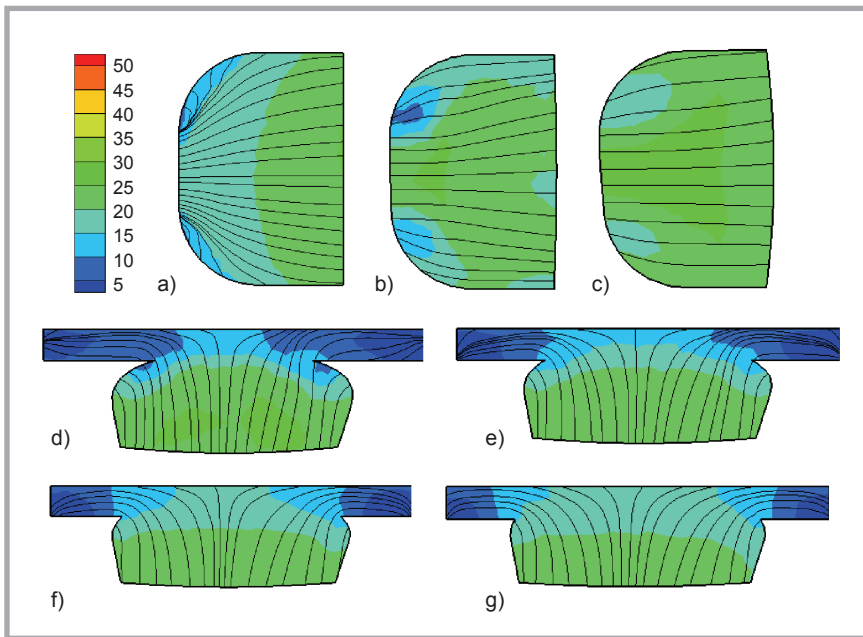


Figure 9. Velocity streamlines and contours of the airflow in the transport channel at cross-section: a) $y = 32$ mm, b) $y = 30$ mm, c) $y = 28$ mm, d) $x = 25$ mm, e) $x = 26$ mm, f) $x = 27$ mm and g) $x = 28$ mm.

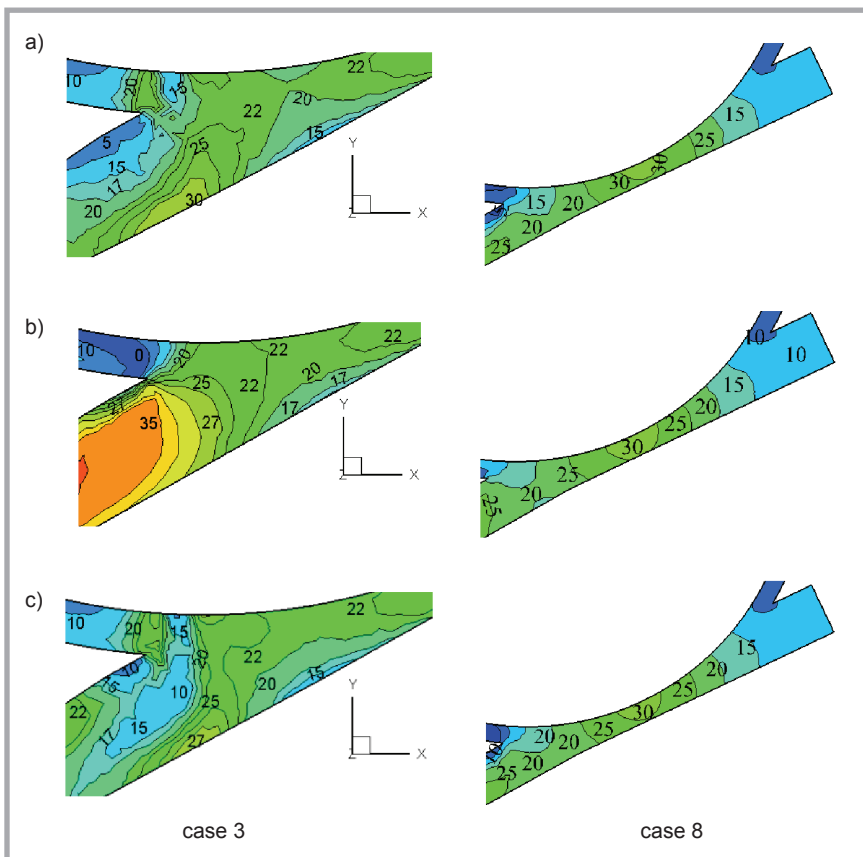


Figure 10. Velocity contours of the transport channel in cases 2 and 8 at cross sections: a) $z = -10$ mm, b) $y = -6$ mm and c) $y = -2$ mm. (unit: m/s).

of the bypass channel are 6×16 mm². The bypass channel is open to the atmosphere, and therefore the external air will flow into the bypass channel due to the pressure difference between

the rotor and the external environment. This would lead to an increase in mass flow from the bypass channel and, consequently, in the air velocity in the fibre transport channel, which is expected to

improve the airflow streamlines for the fibres.

Based on the mathematical model established in the section “Theoretical and mathematical model”, case 8, where the bypass channel inlet absolute pressure is set as 101000 Pa, is calculated, and the results are compared with those of case 3.

Effect of the bypass channel

The velocity streamlines and contours of the airflow along the cross-section of the transport channel inlet with a bypass channel as an air supply channel are illustrated in **Figure 9**.

It can be observed that the velocity streamlines at cross sections $y = 32$ mm, 30 mm, and 28 mm are smooth, and no vortices are generated, as compared to case 3 in **Figure 2**. Having the bypass channel for extra air supply, the air velocity at the transport channel inlet, especially in the fibre separation area, is increased as compared to that in the traditional transport channel. The velocity distribution of the transport channel cross sections in cases 1 to 7, shown in **Figures 2, 4 and 6**, is uneven, while a relatively uniform one is observed in the modified transport channel in **Figure 9**. Notice as well that vortices do not exist in the x cross sections of the transport channel, indicating that the vortices appearing on two sides of the conventional transport channel inlet can be eliminated with the introduction of a bypass. The velocity distribution and streamlines of the modified transport channel are favourable for fibre transportation, since the risk of fibre bending due to the vortices is reduced.

Figure 10 illustrates a comparison of the velocity contours in the fibre separation area between case 3 (traditional transport channel) and case 8 (modified transport channel). In these two cases, the opening roller speeds are both 6000 rpm, that is to say the circumferential velocity of the opening roller is 19.16 m/s. The individual fibres have the same velocity with the roller since they are held by the opening roller pins. The ratio of the air velocity around the roller pins to the circumferential velocity of the opening roller is defined as the peeling-drawing ratio, which is a key index indicating the effect of fibre peeling. Generally the peeling-drawing ratio should not be smaller than 1.5, so as to guarantee the success of the peeling process. The higher the

peeling-drawing ratio, the better the fibre configuration when it is peeled from the roller pins. From **Figure 10**, it can be observed that the maximum air velocity in the fibre separation area in case 8 is higher, which is 30 m/s, than that in case 3, which is about 22 m/s. For sections $z = -10$ and -2 mm in case 3, the air velocity experiences a decrease along the transport channel, while in case 8 it gradually increases. For the latter, it is more beneficial to the drawing process of individual fibres, consequently improving fibre straightness.

The improvement of the streamlines of the airflow along the transport channel may be due to the following reasons.

- (1) The mass flow at the rotor outlet is equal to that from the rotor spinning channel inlet per unit time. For the traditional rotor spinning unit, the overall mass flow directed to the rotor is from the trash extraction chute (the one from the yarn guiding mouth is too little to ignore). When the bypass channel was added as an air supply channel, the overall mass flow to the rotor is supplied by the bypass channel, except that from the trash extraction chute. Therefore the mass flow from the trash extraction chute would be decreased, leading to a reduction in mass flow in the opening roller chamber anticlockwise, which could be considered as the main cause of the transport channel inlet vortices.
- (2) As the bypass channel is located in the tangential direction of the long axis of the transport channel, the external atmosphere flows into the transport channel tangentially. This air stream combines with that from the opening roller cavity, forming a stronger main air stream flowing into the transport channel, which would lower the inertia of the air stream from the opening roller cavity anticlockwise. Therefore the risk of forming a vortex is reduced, or even eliminated, and the air velocity in the fibre separation area is increased accordingly.

The advantages of removing the vortices are significant. The fibres escaping from the opening roller pins will not be affected by the vortices. Furthermore the effective width, defined as the width of a cross section containing forward flow, is increased. Therefore the orientation of fibres is improved, and hence yarn properties.

Conclusions

In this paper, a three-dimensional computational model is developed to investigate the effect of the characteristic number of the transport channel on airflow patterns. The effect of a bypass channel located on the longer side of the transport channel as an extra air supply channel is also evaluated. According to the above analysis, the following conclusions may be drawn:

1. The effect of the characteristic number λ on the airflow dynamics of the transport channel is complex. It mainly depends on the transport channel length and its inlet area. On the whole, with an increase in the characteristic number, the vortices generated at the transport channel inlet increase. For a constant characteristic number, it is recommended that the transport channel length and inlet area be decreased simultaneously.
2. As the transport channel length increases, the vortices generated on both sides of the transport channel inlet decrease. The air velocity in the transport channel inlet centre region increases slightly. Increasing the transport channel inlet area will lead to a significant increase in the vortices and a noticeable decrease in the air velocity of the centre area of the transport channel inlet. The transport channel inlet area has a greater effect on the airflow characteristics of the transport channel than the transport channel length.
3. The bypass channel plays an important role in improving the airflow streamlines of the transport channel. Due to the pressure difference between the rotor and the outside environment, external air flows into the transport channel from the bypass channel. The vortices are reduced significantly, and the air velocity in the fibre separation area is higher and more uniform.

References

1. Das A, Alagirusamy R. 3 – Fundamental principles of open end yarn spinning. In C. A. Lawrence (Ed.), *Advances in yarn spinning technology, woodhead publishing series in textiles*, UK: Woodhead Publishing, 2010: 79-101.
2. Kong LX, Platfoot RA. Computational Two-Phase Air/Fiber Flow Within Transfer Channels of Rotor Spinning Machines. *Textile Research Journal* 1997; 67(4): 269-278.
3. Smith AC, Roberts WW. Straightening of Crimped and Hooked Fibers in Co-

- verging Transport Ducts: Computational Modeling. *Textile Research Journal* 1994; 64(6): 335-344.
4. Kong LX, Platfoot RA. Fibre transportation in confined channel with recirculations. *Computers and Structures* 2000; 78: 237-245.
5. Kong LX, Platfoot RA. Two-Dimensional Simulation of Air Flow in the Transfer Channel of Open-End Rotor Spinning Machines. *Textile Research Journal* 1996; 66(10): 641-650.
6. Lin HT, Zeng YC, Wang J. Computational simulation of air flow in the rotor spinning unit. *Textile Research Journal* 2015; 86(2): 115-126.
7. Xiao M, Dou HS, Wu C. Critical rotating speed of rotor cup in an air suction open-end spinning machine. *Textile Research Journal* 2016; 87(13): 1593-1603.
8. Koç E, Lawrence CA. Mechanisms of wrapper fibre formation in rotor spinning: An experimental approach. *The Journal of the Textile Institute* 2006; 97(6): 483-492.
9. Lawrence CA, Chen KZ. A Study of the Fibre-transfer-channel Design in Rotor-spinning. Part II: Optimization of the Transfer-channel Design. *The Journal of the Textile Institute* 1988; 79(3): 393-408.
10. Lawrence, C.A., and K.Z. Chen. A Study of the Fibre-transfer-channel Design in Rotor-spinning. Part I: The Fibre Trajectory. *The Journal of the Textile Institute*, 1988; 79(3): 367-392.
11. Eskandarnejad S. A study of fiber behaviour in the transfer zone of an open-end spinning system. PhD Thesis, University of Manchester, UK, 1991.
12. Seyed S, Eskandarnejad S, Emamzadeh A. Effect of geometry of end of the fibre transport channel with slotted exit on rotor spun yarn quality. *The Journal of The Textile Institute* 2015; 106(5): 564-570.
13. Wang J, Yan J X, Liang Y, Yuze Z, Wei G, Ting F. Dual Feed Carding Device. Chinese Patent CN103911696A. 2014.
14. Akankwasa NT, Lin HT, Zhang YZ, Wang J. Numerical simulation of three-dimensional airflow in a novel dual-feed rotor spinning box. *Textile Research Journal* 2016; 88(3): 237-253.
15. Akankwasa NT, Lin HT, Wang J. Evaluation of the dual-feed rotor spinning unit based on airflow dynamics and blended yarn properties. *The Journal of The Textile Institute* 2017; 108(11): 1985-1996.
16. Zhang LH, Zhang BX. A Study of Fiber Transfer Channel in Rotor Spinning. *Journal of China Textile University* 1991; 17(6): 16-26.
17. Lin HT, Bergada JM, Zeng YC, Akankwasa NT, Zhang Z, Wang J. Rotor spinning transfer channel design optimization via computational fluid dynamics. *Textile Research Journal* 2018; 88(11): 1244-1262.

Received 25.07.2018 Reviewed 04.12.2018